Original Article | Neuroimaging and Head & Neck

eISSN 2005-8330
https://doi.org/10.3348/kjr.2021.0323
Korean J Radiol 2022;23(1):89-100

Korean Journal of Radiology
KJR

Prediction of Cognitive Progression in Individuals with Mild Cognitive Impairment Using Radiomics as an Improvement of the ATN System: A Five-Year Follow-Up Study

Rao Song[1]*, Xiaojia Wu[1]*, Huan Liu[2], Dajing Guo[1], Lin Tang[1], Wei Zhang[1], Junbang Feng[3], Chuanming Li[1]

[1]Department of Radiology, the Second Affiliated Hospital of Chongqing Medical University, Chongqing, China; [2]GE Healthcare, Shanghai, China; [3]Department of Radiology, Chongqing Emergency Medical Center, Chongqing, China

Objective: To improve the N biomarker in the amyloid/tau/neurodegeneration system by radiomics and study its value for predicting cognitive progression in individuals with mild cognitive impairment (MCI).

Materials and Methods: A group of 147 healthy controls (HCs) (72 male; mean age ± standard deviation, 73.7 ± 6.3 years), 197 patients with MCI (114 male; 72.2 ± 7.1 years), and 128 patients with Alzheimer's disease (AD) (74 male; 73.7 ± 8.4 years) were included. Optimal A, T, and N biomarkers for discriminating HC and AD were selected using receiver operating characteristic (ROC) curve analysis. A radiomics model containing comprehensive information of the whole cerebral cortex and deep nuclei was established to create a new N biomarker. Cerebrospinal fluid (CSF) biomarkers were evaluated to determine the optimal A or T biomarkers. All MCI patients were followed up until AD conversion or for at least 60 months. The predictive value of A, T, and the radiomics-based N biomarker for cognitive progression of MCI to AD were analyzed using Kaplan-Meier estimates and the log-rank test.

Results: The radiomics-based N biomarker showed an ROC curve area of 0.998 for discriminating between AD and HC. CSF Aβ42 and p-tau proteins were identified as the optimal A and T biomarkers, respectively. For MCI patients on the Alzheimer's continuum, isolated A+ was an indicator of cognitive stability, while abnormalities of T and N, separately or simultaneously, indicated a high risk of progression. For MCI patients with suspected non-Alzheimer's disease pathophysiology, isolated T+ indicated cognitive stability, while the appearance of the radiomics-based N+ indicated a high risk of progression to AD.

Conclusion: We proposed a new radiomics-based improved N biomarker that could help identify patients with MCI who are at a higher risk for cognitive progression. In addition, we clarified the value of a single A/T/N biomarker for predicting the cognitive progression of MCI.

Keywords: *Alzheimer's disease; Mild cognitive impairment; Biomarker; ATN; Radiomics; Prediction*

INTRODUCTION

Alzheimer's disease (AD) is the leading cause of dementia, and the risk increases with age [1]. The impairment of cognitive function and behavior occurring in AD is progressive and unremitting, requiring long-term care and causing a considerable economic burden on the family. It is estimated that by 2020, the total expenditure of all patients with AD and other types of dementia will be $305 billion [2]. AD has a distinct pathology associated with

Received: April 21, 20219 **Revised:** August 19, 2021 **Accepted:** August 24, 2021
*These authors contributed equally to this work.
Corresponding author: Chuanming Li, MD, Department of Radiology, the Second Affiliated Hospital of Chongqing Medical University, No. 74 Linjiang Rd, Yuzhong District, Chongqing 400010, China.
• E-mail: lichuanming@hospital.cqmu.edu.cn

the accumulation of amyloid and tau proteins in the brain. In the early stages of the disease, there is no cognitive impairment; however, neuropathological changes have emerged. Timely treatment may be effective before the disease reaches an irreversible degenerative state [3,4]. Based on the changes in neuropathology, the 2018 National Institute of Aging and Alzheimer's Association proposed the amyloid/tau/neurodegeneration (ATN) classification scheme to redefine AD using biomarkers other than clinical symptoms [5]. Individuals can be classified as abnormal (+) or normal (-) for A, T, and N, resulting in eight different ATN profiles.

Cerebrospinal fluid (CSF) examination or brain imaging such as MRI or PET can be used to identify ATN biomarkers. Owing to its high cost and radioactivity, the application of PET is limited. Accessible methods, such as CSF and MRI, are most widely used in clinical practice. However, most previous studies have only used a single indicator in parts of the brain, such as the volume of the hippocampus [6-8], the rating of medial temporal lobe atrophy [9-11], or the thickness of the cerebral cortex [6,8] to assess the N biomarker. In fact, areas with neural damage caused by AD in the brain include the entire cortex and subcortical nuclei. For example, Lehmann et al. [12] reported a decreased cortical thickness in the bilateral posterior cingulate gyrus, precuneus, and posterior parietal lobes in patients with AD. Subcortical nuclei, such as the putamen, thalamus, and basal ganglia, can also undergo significant atrophy related to cognitive impairment [13,14]. Therefore, it is of great significance to comprehensively investigate the structural changes in the brain and obtain a sensitive and accurate N biomarker to further improve the ATN system.

Mild cognitive impairment (MCI), a transitional state between normal cognition and AD, has always been a focus of attention. Indeed, it is estimated that approximately 60% of MCI cases will progress to dementia during the 3-year follow-up, with this rate increasing to 80% at the 4-year follow-up [15,16]. Previously, it has been reported that MCI patients with different ATN combinations may have different risks of cognitive deterioration [17]. However, the role and predictive value of isolated A/T/N biomarkers in the cognitive progression of MCI remain unclear. In this study, we first analyzed the structural changes in the whole brain using a radiomics approach to establish a new method to evaluate N biomarkers and determine the optimal ATN indicators for distinguishing between healthy controls (HCs) and AD patients. Then, all MCI patients were divided into different groups according to the radiomics-based ATN groups and were followed for five years to investigate the value of isolated A/T/N biomarkers for predicting cognitive progression.

MATERIALS AND METHODS

Participants

The data used in this study were downloaded from the Alzheimer's Disease Neuroimaging Initiative (ADNI) website (adni.loni.usc.edu). The ADNI study was approved by an ethics committee on human experimentation at each institution, and written informed consent was obtained from all participants. In total, 147 HCs, 197 patients with MCI, and 128 patients with AD from ADNI-GO and ADNI-2 were included. The patients with AD satisfied the criteria by National Institute of Neurological and Communicative Disorders and Stroke (NINCDS)/Alzheimer's Disease and Related Disorders Association (ADRDA) for probable AD [18,19]. The participants with MCI reported a subjective memory concern; however, they showed no significant impairment in other cognitive domains, everyday activities were substantially preserved, and there were no signs of dementia. The HC subjects showed no signs of depression, MCI, or dementia. All participants had complete demographic, clinical, and laboratory characteristics and MR images of T1-weighted imaging at the baseline of data collection. The MCI subjects were followed up for 6–60 months, with a follow-up interval of 6–12 months in the first 3 years and 12 months after 3 years. Among them, 100 patients progressed to dementia, and the remaining 97 patients remained stable during the follow-up period. Participants who temporarily progressed from MCI to AD and returned to MCI during the entire observation period were not considered to have cognitive progression in this study. Figure 1 shows the workflow of the study.

Clinical and CSF Characteristics

Clinical and CSF information was directly collected from the ADNI assessment files. Demographic characteristics included age, sex, education level, alcohol abuse, body mass index, and prevalence of apolipoprotein (APOE) ε4. Eleven neuropsychological scales were adopted to evaluate cognitive function at baseline, including the Mini-Mental State Examination (MMSE), Alzheimer's Disease Assessment Scale-Cognitive subscale (ADAS-Cog), Clinical Dementia Rating (CDR), Functional Activities Questionnaire (FAQ), Geriatric

https://doi.org/10.3348/kjr.2021.0323

Korean Journal of Radiology
KJR

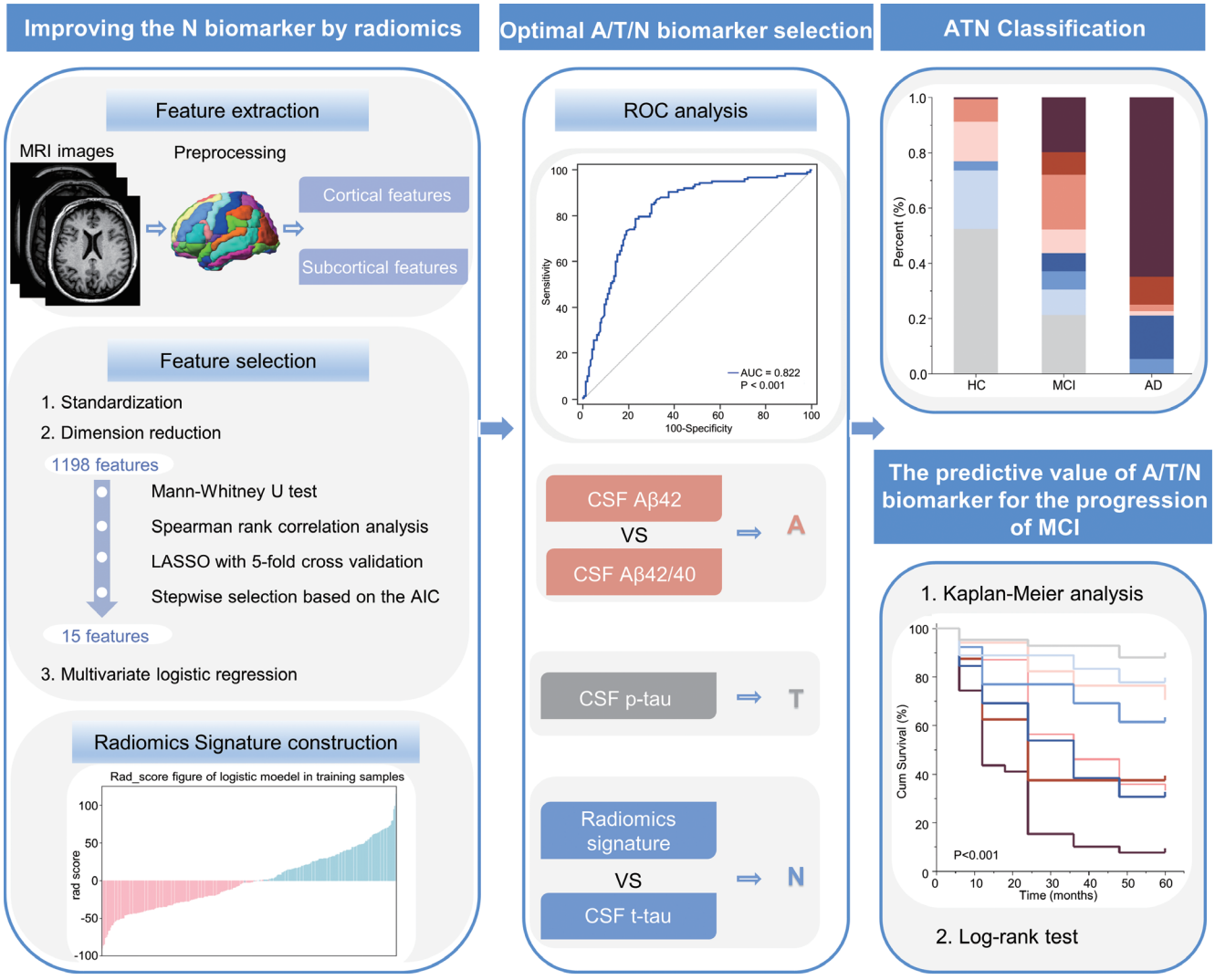

Fig. 1. The working flow chart of this study. AD = Alzheimer's disease, AIC = Akaike information criterion, ATN = amyloid/tau/neurodegeneration, AUC = area under the curve, Aβ = amyloid-β, CSF = cerebrospinal fluid, HC = healthy control, LASSO = least absolute shrinkage and selection operator, MCI = mild cognitive impairment, p-tau = phosphorylated tau, ROC = receiver operating characteristic, t-tau = total tau

Depression Scale (GDS), Rey Auditory Verbal Learning Test (RAVLT), and Animal Fluency Test (AFT). CSF characteristics included CSF Aβ42, Aβ40, p-tau, and t-tau protein levels.

MRI Acquisition and Radiomics Feature Extraction

Structural MRI was performed using a three-dimensional magnetization prepared rapid gradient echo sequence or equivalent scanning scheme on 3T scanners (261 cases from Siemens Medical Solutions, 128 cases from General Electric Healthcare, and 83 cases from Philips Medical Systems). MRI data acquisition techniques were standardized across different scanners according to the ADNI protocol (see http://adni.loni.ucla.edu/research/protocols/mri-protocols/). Detailed imaging parameters were available from the ADNI website (http://adni.loni.usc.edu/methods/documents/). FreeSurfer software (version 6.0; http://surfer.nmr.mgh.harvard.edu/) was used. FreeSurfer has been proven to have good stability in brain segmentation and feature extraction [20]. During this study, the computing hardware, operating system, and FreeSurfer version remain unchanged and run automatically without user intervention. Briefly, the procedure included motion correction, removal of the skull, Talairach transformation, gray/white matter segmentation, intensity normalization, topology correction, surface deformation, inflation, registration, and parcellation. The whole cortex was divided into 146 cortical regions according to the Destrieux Atlas. Indicators including surface area, average thickness, standard deviation of thickness, integrated rectified Gaussian curvature, integrated rectified mean curvature, intrinsic curvature index, folding index,

https://doi.org/10.3348/kjr.2021.0323

and gray matter volume were obtained from each cortical region. In addition, 14 regions were obtained from the subcortical segmentation according to the Desikan-Killiany Atlas, including the bilateral thalamus, caudate, putamen, pallidum, hippocampus, amygdala, and nucleus accumbens. The volume of each subcortical structure was then determined. Finally, 1198 image features were extracted.

Radiomics Feature Selection and Model Construction

Standardization in the feature domain was performed prior to the feature selection. First, abnormal values were replaced by the median. The features were then standardized to eliminate the influence of the dimension.

Dimension reduction was performed, as shown in Figure 1. Mann-Whitney U tests were first introduced to select features with $p < 0.05$, as potentially informative features. Second, Spearman correlation analysis was used to identify redundant features. Highly correlated features were eliminated if the correlation coefficient was higher than 0.9. Third, the least absolute shrinkage and selection operator (LASSO) regression algorithm was applied to select features with 5-fold cross-validation. LASSO is a shrinkage and selection method for linear regression. It minimizes the usual sum of squared errors, with a bound on the sum of the absolute values of the coefficients. Regularization methods estimate the value of the regression coefficients β by minimizing the following objective function:

$$min_\beta \left(\frac{1}{n} \sum_{i=1}^{n} (y_i - x_i^T \beta)^2 + \lambda \|\beta\|_1 \right)$$

where λ is the regression coefficient operating on the standardized covariate i, and λ is a penalty term (also known as a tuning parameter), which controls the value of shrinkage. Fourth, backward stepwise selection based on the Akaike information criterion was applied to remove features that were not significant. Finally, the most powerful radiomics features were utilized to construct a radiomics model based on logistic regression. The likelihood ratio test with backward step-down selection was applied to the multivariate logistic regression model. Then, the radiomics score (rad-score) of each individual was calculated through a linear combination of selected features multiplied by their respective coefficients.

Radiomics Model Evaluation and Optimal CSF Biomarker Screening

Logistic regression leveraging 5-fold cross-validation was employed to assess the performance of the radiomics model. This method randomly separated the data into five subsets and used one subset as the validation set and the remaining subsets as the training set. This process was repeated until all subsets were utilized. The area under the curve (AUC), sensitivity, and specificity were used to assess the performance of the radiomics model. For each CSF biomarker, a receiver operating characteristic (ROC) curve was generated, and Youden's index was calculated to determine the optimal biomarker and cutoff value for discriminating between HCs and AD patients.

Statistical Analysis

Statistical analysis was performed using IBM SPSS Statistics for Windows, version 24.0, (IBM Corp.). Frequency (%) and mean ± standard deviation were used to describe categorical variables and normally distributed continuous variables. The median with interquartile range was used to describe non-normally distributed continuous variables. One-way analysis of variance and Kruskal-Wallis tests were performed for statistical analysis of continuous variables. When a statistically significant overall difference was detected, pairwise comparisons between groups were conducted using Tukey or Nemenyi post-hoc analysis for the correction of multiple comparisons. The chi-square test and Fisher's exact test were used for statistical analysis of categorical variables. Cognitive progression of MCI patients with different ATN profiles was estimated using the Kaplan-Meier method, and any differences between different ATN profile groups were evaluated with a stratified log-rank test for overall comparisons and pairwise comparisons adjusted by Bonferroni correction.

RESULTS

Participant Characteristics at Baseline

The baseline characteristics of the participants are shown in Table 1 and Supplementary Table 1. There were no significant group differences in age, sex, or alcohol abuse among the three groups. For the neuropsychological scales, all groups differed significantly between each other regarding MMSE, ADAS-Cog11, ADAS-Cog13, CDR, FAQ, RAVLT immediate, RAVLT learning, RAVLT percent forgetting, and AFT (all $p < 0.05$). CSF biomarkers were significantly different between the HC, MCI, and AD groups (all $p < 0.05$). The AD group contained the lowest Aβ42 content and the highest p-tau and t-tau content. The APOE ε4 also varied

https://doi.org/10.3348/kjr.2021.0323

Korean Journal of Radiology
KJR

Table 1. Baseline Characteristics of HC, MCI, and AD Groups

	HC (n = 147)	MCI (n = 197)	AD (n = 128)	*P*	Post-Hoc Test
Age, year	73.7 ± 6.3	72.2 ± 7.1	73.7 ± 8.4	0.106	
Sex, male	72 (49.0)	114 (57.9)	74 (57.8)	0.200	
Education, year	16.59 ± 2.53	16.20 ± 2.75	15.48 ± 3.06	0.004	b
Alcohol abuse	7 (4.8)	9 (4.6)	10 (7.8)	0.407	
BMI	27.21 ± 4.28	27.82 ± 5.08	25.89 ± 5.10	0.002	c
APOE ε4 carrier	40 (27.2)	105 (53.3)	86 (67.2)	< 0.001	a, b, c
MMSE	29.08 ± 1.15	27.68 ± 1.81	23.35 ± 2.05	< 0.001	a, b, c
ADAS-Cog11	5.87 ± 3.10	10.75 ± 4.78	20.35 ± 6.92	< 0.001	a, b, c
ADAS-Cog13	9.05 ± 4.49	17.32 ± 7.23	30.60 ± 8.13	< 0.001	a, b, c
CDR	0.00 (0.00, 0.00)	0.50 (0.50, 0.50)	1.00 (0.50, 1.00)	< 0.001	a, b, c
FAQ	0.00 (0.00, 0.00)	2.00 (0.00, 5.50)	13.00 (8.00, 18.00)	< 0.001	a, b, c
GDS	0.00 (0.00, 1.00)	2.00 (1.00, 3.00)	1.00 (1.00, 2.00)	< 0.001	a, b
RAVLT immediate	46.22 ± 10.18	33.42 ± 9.67	22.52 ± 6.93	< 0.001	a, b, c
RAVLT learning	5.90 ± 2.39	4.07 ± 2.62	1.82 ± 1.69	< 0.001	a, b, c
RAVLT forgetting	3.84 ± 2.67	4.96 ± 2.41	4.39 ± 1.56	< 0.001	a
RAVLT percent forgetting	36.00 ± 27.32	65.28 ± 31.12	88.69 ± 20.06	< 0.001	a, b, c
AFT	21.54 ± 5.43	16.85 ± 4.98	12.30 ± 4.68	< 0.001	a, b, c

a, HC vs. MCI; b, HC vs. AD; c, MCI vs. AD. Data are shown as the mean ± standard deviation, number (%), or median (interquartile range). Chi-square tests with Bonferroni correction were used for analysis of sex, alcohol abuse, and APOE ε4 carriers. One-way analysis of variance with Tukey's post hoc test was used for analysis of education, BMI and AFT. The Kruskal-Wallis H test followed by the Nemenyi test was used for analysis of other continuous variables. AD = Alzheimer's disease, ADAS-Cog = Alzheimer's Disease Assessment Scale-Cognitive subscale, AFT = Animal Fluency Test, APOE = apolipoprotein, BMI = body mass index, CDR = Clinical Dementia Rating, FAQ = Functional Activities Questionnaire, GDS = Geriatric Depression Scale, HC = healthy control, MCI = mild cognitive impairment, MMSE = Mini-Mental State Examination, RAVLT = Rey Auditory Verbal Learning Test

among the different groups (all $p < 0.05$), with the AD group containing the highest number of APOE ε4 carriers.

Radiomics Model Construction and Performance Evaluation

Using the Mann-Whitney U test and Spearman analysis, 503 features were obtained from among 1198 features. These features were then reduced to 46 with nonzero coefficients using the LASSO method (Fig. 2A, B). After the stepwise selection based on the Akaike information criterion, 15 optimal features were obtained to build the radiomics model. The optimal features and their coefficients are shown in Figure 2C. The ROC curve of the radiomics model is shown in Figure 2D. The AUC with 5-fold nested cross-validation was 0.998 (sensitivity, 0.969; specificity, 0.973).

Optimal A/T/N Biomarkers and the Frequency of Different ATN Profiles among HC, MCI, and AD Subjects

As shown in Figures 3A and 3B, the AUC of CSF Aβ42 was 0.822, which was higher than that of the CSF Aβ42/Aβ40 ratio (0.813) and was considered the optimal A biomarker. Similarly, the radiomics model showed a higher AUC of 0.998 (Fig. 2D) than CSF t-tau (0.795; Fig. 3D) and was chosen as the optimal N biomarker. According to the ATN classification scheme, we classified each participant using the three binary categories: A+ referring to Aβ pathology (CSF Aβ42 levels ≤ 952 pg/mL), T+ referring to pathologic p-tau (CSF p-tau > 24.38 pg/mL), and N+ referring to the neurodegeneration radiomics biomarker (rad-score > 0.4561).

Stratified by cognitive stage, A-T-N- was the most common ATN profile in HCs. In contrast, the A-T+N+, A+T-N+ and A+T+N+ profiles were the least common profiles in HC, accounting for less than 1%. Among MCI individuals, the group with the highest proportion was A-T-N- (21.3%), followed by A+T+N- (19.8%) and A+T+N+ (19.8%). The prevalence of A+T+N+ was dominant in patients with AD, with a high proportion (64.8%). In addition, no participant showed a biomarker combination of A-T-N- or A-T-N+ in AD (Table 2).

Predictive Value of a Single A/T/N Biomarker for the Cognitive Progression of MCI Individuals at Five-Year Follow-Up

During the five-year follow-up period, the cognitive progression rates of different ATN profiles varied. The A+T+N+ profile and A-T-N- profile showed the highest

 https://doi.org/10.3348/kjr.2021.0323

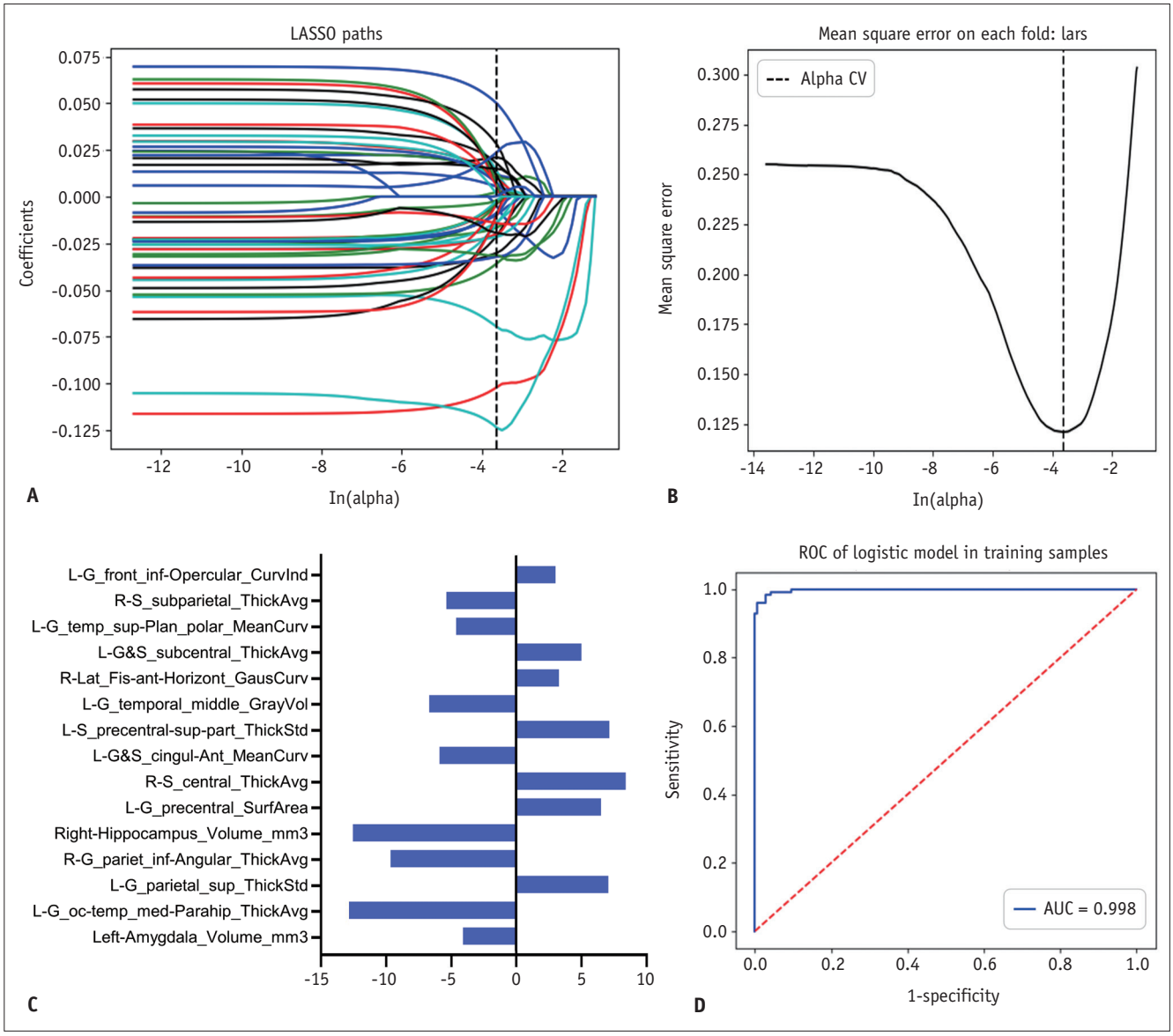

Fig. 2. Radiomics feature selection and model construction.
A. The tuning parameter λ selection in the LASSO model used 5-fold CV via the minimum criteria. Mean square error was plotted vs. log (λ). The dotted vertical lines were drawn at the optimal values using the minimum criteria and the 1-standard error criteria. **B.** LASSO coefficient profiles of the radiomic features. A vertical line was drawn at the value selected using 5-fold CV in the ln(alpha) sequence, and 15 non-zero coefficients are indicated. **C.** A histogram displays the 15 optimal radiomics features for AD diagnosis from HCs and their coefficients. **D.** The ROC curve of the radiomics model for discrimination between AD patients and HCs. AD = Alzheimer's disease, AUC = area under the curve, CV = cross validation, HC = healthy control, LASSO = least absolute shrinkage and selection operator, ROC = receiver operating characteristic

(92.3%) and lowest (11.9%) progression rates, respectively. For the Alzheimer's continuum, there was no significant difference in the progression rate of the A+T-N- and A-T-N- profiles ($p > 0.05$). The A+T+N- and A+T-N+ profiles both had significantly higher progression rates than the A+T-N- patients (both $p < 0.05$). The progression rate of the A+T+N+ profile was significantly higher than that of the A+T+N- ($p < 0.001$) or A+T-N+ profile ($p < 0.05$). For the MCI of SNAP, patients with A-T-N+ ($p < 0.05$) and A-T+N+ ($p < 0.001$) profiles showed significantly higher progression rates than those with A-T-N-. There was no significant difference in the progression rates of the A-T+N- and A-T-N- profiles ($p > 0.05$) (Table 3, Fig. 4).

DISCUSSION

Neurodegeneration is a characteristic of pathological changes in AD and is closely related to symptoms [21].

https://doi.org/10.3348/kjr.2021.0323

Korean Journal of Radiology
KJR

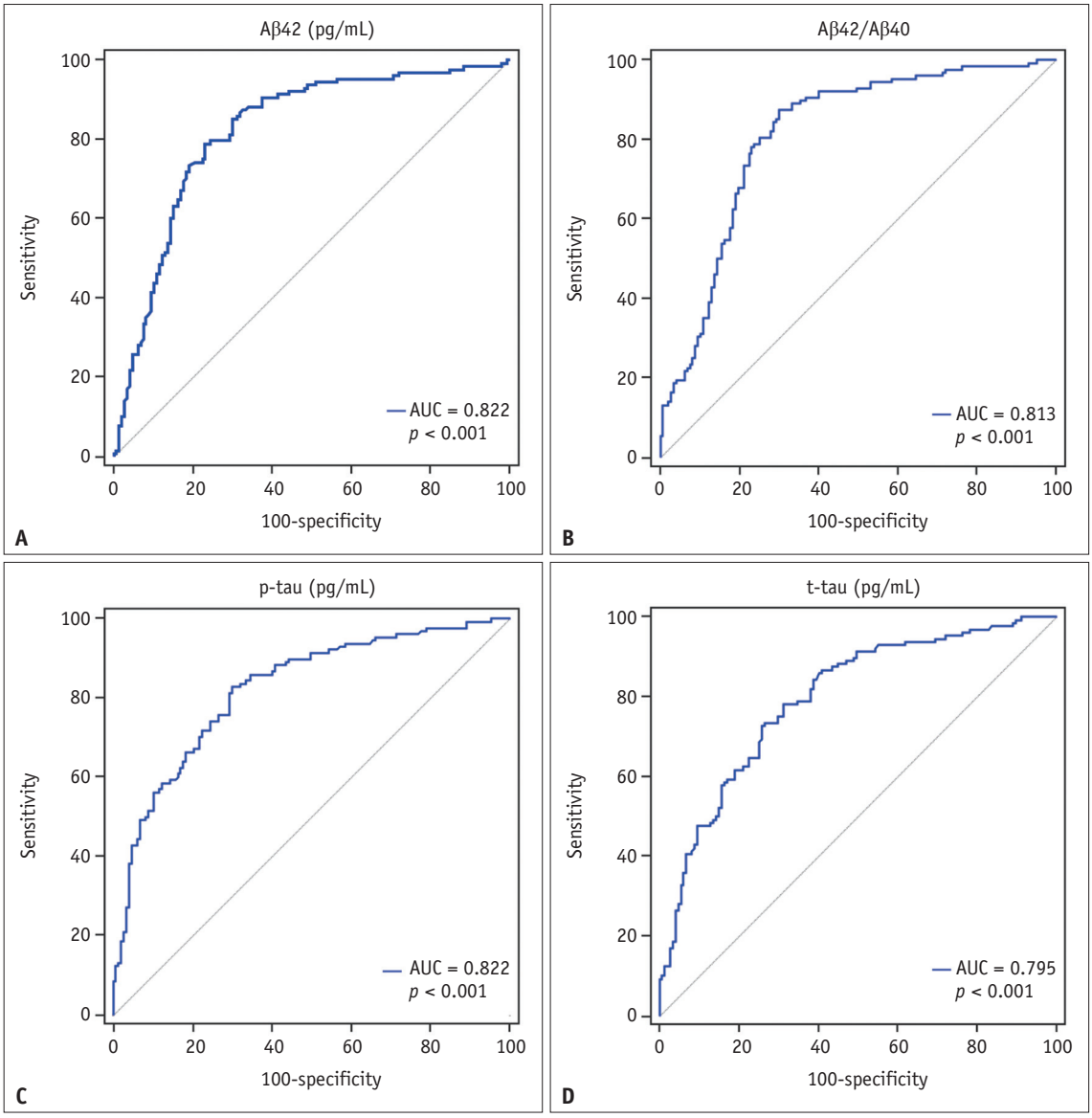

Fig. 3. ROC curves of the CSF biomarkers for discrimination between Alzheimer's disease and healthy controls.
A. ROC curve of CSF Aβ42. **B.** ROC curve of CSF Aβ42/Aβ40. **C.** ROC curve of CSF p-tau. **D.** ROC curve of CSF t-tau. AUC = area under the curve, Aβ = amyloid-β, CSF = cerebrospinal fluid, p-tau = phosphorylated tau, ROC = receiver operating characteristic, t-tau = total tau

Brain atrophy can reflect the degree of neurodegeneration, and can be detected using MRI. Most previous studies only used a single indicator of the volume or thickness of AD-specific regions, such as the hippocampus and temporal lobe, to evaluate N biomarkers [6-11]. Many other important brain areas and features have been ignored. As a new discipline, radiomics can extract a large number of high-throughput imaging features from traditional medical images and use machine learning to establish an artificial intelligence model to improve the accuracy of identification. In recent years, radiomics has been widely used in the diagnosis, classification, and prognosis prediction of neurodegenerative diseases, such as AD and Parkinson's disease [22-26]. To our knowledge, this is the first time that a radiomics method based on MRI of the whole brain has been used to evaluate N biomarkers. The sensitivity and specificity of the discrimination between HCs and AD were 0.969 and 0.973, respectively, which were higher than the hippocampal volume (sensitivity, 0.673; specificity, 0.803) or brain mean cortical thickness (sensitivity, 0.833; specificity, 0.859) reported previously [6]. Different MRI indices can reflect brain atrophy from different aspects. Our combined multiple indicators included cortical thickness, cortical area, cortical curvature, and subcortical volume

 https://doi.org/10.3348/kjr.2021.0323

of several brain regions, which could comprehensively reflect degenerative changes in the brain. Most radiomics features were located in the temporal, frontal, and parietal cortices. Structural changes in these cortical regions have been reported in patients with AD pathology and have been shown to be associated with disease progression [27-29]. In typical cases of AD, abnormalities of amyloid plaques or neurofibrillary tangles usually first appear in regions of the temporal lobes and hippocampus and progressively spread to the frontal lobes and other areas of the cortex [30]. The parietal lobe is considered to be a multimodal area of cognition. Parietal lobe dysfunction may be one of the causes of cognitive dysfunction in early AD [31]. The volume of the amygdala is also a retained feature. Previous studies have reported that a decrease in amygdala volume is related to cognitive dysfunction and can be used as a marker of dementia severity in patients with AD [32,33]. In the ATN system, neurodegeneration can be evaluated using CSF t-tau or brain imaging. In this study, the accuracy of the radiomics model was significantly higher than that of the CSF t-tau. A possible rationale is that brain atrophy on MRI reflects the cumulative loss and damage of nerve cells, while t-tau in CSF only reflects the damage of neurons at a certain time point.

According to the ATN system, excessive Aβ deposition

Table 2. The Frequency of the 8 ATN Profiles and 3 Biomarker Categories in HC, MCI, and AD Groups

	HC (n = 147)	MCI (n = 197)	AD (n = 128)
ATN profiles			
A-T-N-	77 (52.4)	42 (21.3)	0
A-T+N-	31 (21.1)	18 (9.1)	0
A-T-N+	5 (3.4)	13 (6.6)	7 (5.5)
A-T+N+	0	13 (6.6)	20 (15.6)
A+T–N-	21 (14.3)	17 (8.6)	2 (1.6)
A+T+N-	12 (8.2)	39 (19.8)	3 (2.3)
A+T-N+	0	16 (8.1)	13 (10.2)
A+T+N+	1 (0.7)	39 (19.8)	83 (64.8)
Biomarker categories			
Normal	77 (52.4)	42 (21.3)	0
SNAP	36 (24.5)	44 (22.3)	27 (21.1)
Alzheimer continuum	34 (23.1)	111 (56.3)	101 (78.9)

Data are shown as the number (%). AD = Alzheimer's disease, ATN = amyloid/tau/neurodegeneration, HC = healthy control, MCI = mild cognitive impairment, SNAP = suspected non-Alzheimer pathology

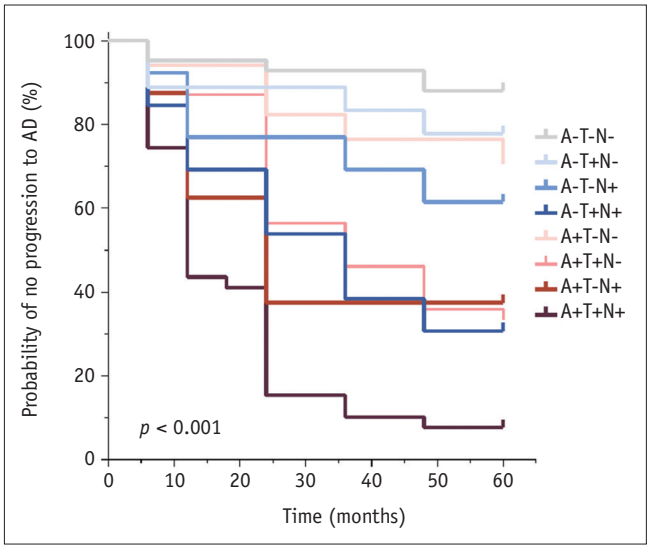

Fig. 4. Kaplan-Meier curves illustrate the 5-year probability of no progression to AD of eight ATN profiles of mild cognitive impairment patients. AD = Alzheimer's disease, ATN = amyloid/tau/neurodegeneration

Table 3. The 1-, 3-, 5-Year Probabilities of No Cognitive Progression and 5-Year Cumulative Progression Rates of 8 ATN Profiles of Mild Cognitive Impairment Patients

ATN Profile	N	Probability of Remaining Without Progression to AD			5-Year Progression (%)	$P < 0.05$*
		1-Year (%)	3-Year (%)	5-Year (%)		
A-T-N-	42	95.2	92.9	88.1	11.9	a, b, c, d, e
A-T+N-	18	88.9	83.3	77.8	22.2	f, g, h, i
A-T-N+	13	92.3	69.2	61.5	38.5	j
A-T+N+	13	84.6	53.8	30.8	69.2	k, l
A+T-N-	17	94.1	76.5	70.6	29.4	m, n, o
A+T+N-	39	92.3	56.4	33.3	66.7	p
A+T-N+	16	87.5	37.5	37.5	62.5	q
A+T+N+	39	74.4	15.4	7.7	92.3	

a, A-T-N- vs. A-T-N+; b, A-T-N- vs. A-T+N+; c, A-T-N- vs. A+T+N-; d, A-T-N- vs. A+T-N+; e, A-T-N- vs. A+T+N+; f, A-T+N- vs. A-T+N+; g, A-T+N- vs. A+T+N-; h, A-T+N- vs. A+T-N+; i, A-T+N- vs. A+T+N+; j, A-T-N+ vs. A+T+N+; k, A-T+N+ vs. A+T-N-; l, A-T+N+ vs. A+T+N+; m, A+T-N- vs. A+T+N-; n, A+T-N- vs. A+T-N+; o, A+T-N- vs. A+T+N+; p, A+T+N- vs. A+T+N+; q, A+T-N+ vs. A+T+N+. A Log rank test was used to compare survival curves among different ATN profiles. AD = Alzheimer's disease, ATN = amyloid/tau/neurodegeneration

https://doi.org/10.3348/kjr.2021.0323

Korean Journal of Radiology
KJR

(A+) is a biomarker of Alzheimer's pathologic changes. In this study, we found that during the 5-year follow-up period of the MCI population, patients with only A biomarker positivity (A+T-N-) clinically progressed at a rate similar to that of patients with the A-T-N- profile. Our findings suggest that the isolated amyloid abnormality (A+) indicates a relatively stable state rather than a sign of accelerated cognitive decline. In fact, amyloid deposition is the initial event of AD-related pathophysiologic change [34], which can last for 5–10 years or longer before the onset of dementia symptoms [35]. Based on the abnormal Aβ plaques, each added biomarker of T or N increases the recent progression rate of MCI patients. Interestingly, a similar risk of progression was observed between A+T+N- and A+T-N+, suggesting that T and N may play equal roles in the prediction of progression. A previous study suggested that A+T+N- and A+T+N+ should be combined into a single group because of their similar baseline characteristics [9]. However, in this study, we found that for A+T+N+ patients, the overall cognitive impairment was more serious, and the risk of cognitive progress was higher. There were significant differences in baseline status and prognosis between the two groups. A+T+N+ patients should receive more attention and timely interventions.

Suspected non-Alzheimer's disease pathophysiology (SNAP) is considered an important category, which refers to individuals without excessive amyloid deposition (A-) but with tau pathology (T+) and/or neurodegenerative disease (N+). SNAP does not represent preclinical AD but includes one or more neuropathological processes or diseases other than AD [36]. During follow-up, we found that the N biomarker evaluated by radiomics features was sensitive in predicting recent cognitive decline in SNAP MCI. A variety of non-AD processes, such as TDP-4, hippocampal sclerosis, or cerebrovascular disease, may contribute to neurodegeneration in these individuals [37,38]. Neuronal loss and atrophy are common features of these diseases. In contrast, most MCI patients with A-T+N- characteristics in SNAP showed clinical stability, indicating that a single CSF p-tau abnormality does not lead to further cognitive decline. This may be because p-tau in SNAP mostly reflects age-related neurofilament angle pathology rather than AD-related neuronal degeneration.

However, there are several limitations to our study. First, the ADNI is a large multicenter database with participants from more than 50 hospitals in the United States and Canada. Heterogeneity between different scanners is inevitable. Second, due to our strict inclusion criteria, the sample size of this study was not large enough. Third, considering the limitations of clinical applications, PET biomarkers were not included. Finally, our analysis was limited to observing the relationship between baseline biomarker status and progression risk of MCI patients, and no longitudinal analysis was performed. Future research should overcome these limitations and analyze the relationship between the dynamic changes in these indicators and the progression of cognitive impairment by using larger samples.

In conclusion, we proposed a new radiomics-based improved N biomarker and clarified the value of a single A/T/N biomarker for predicting the cognitive progression of MCI. For MCI patients on the Alzheimer's continuum, isolated A+ was an indicator of cognitive stability, while abnormalities in T and N, respectively, or simultaneously, indicated a high risk of progression. For MCI patients with SNAP, isolated T+ indicated cognitive stability, while the appearance of the radiomics-based N+ indicated a high risk of progression.

Supplement

The Supplement is available with this article at https://doi.org/10.3348/kjr.2021.0323.

Availability of Data and Material

The datasets generated or analyzed during the study are available from the corresponding author on reasonable request.

Conflicts of Interest

The authors have no potential conflicts of interest to disclose.

Author Contributions

Conceptualization: Chuanming Li, Rao Song, Xiaojia Wu. Data curation: Rao Song, Xiaojia Wu, Lin Tang. Formal analysis: Rao Song, Xiaojia Wu, Huan Liu. Funding acquisition: Chuanming Li, Dajing Guo. Investigation: Rao Song, Xiaojia Wu, Chuanming Li. Methodology: Chuanming Li, Rao Song, Xiaojia Wu, Huan Liu. Project administration: Chuanming Li. Resources: Chuanming Li. Software: Huan Liu, Rao Song. Supervision: Chuanming Li, Dajing Guo. Validation: Rao Song, Xiaojia Wu, Huan Liu. Visualization: Rao Song, Xiaojia Wu, Huan Liu. Writing—original draft: Rao

Song, Xiaojia Wu. Writing—review & editing: Chuanming Li, Rao Song, Xiaojia Wu, Dajing Guo, Lin Tang, Wei Zhang, Junbang Feng.

ORCID iDs
Rao Song
https://orcid.org/0000-0002-7909-3048
Xiaojia Wu
https://orcid.org/0000-0001-6682-9426
Huan Liu
https://orcid.org/0000-0002-6700-962X
Dajing Guo
https://orcid.org/0000-0001-8655-6621
Lin Tang
https://orcid.org/0000-0001-6511-1607
Wei Zhang
https://orcid.org/0000-0002-3933-6009
Junbang Feng
https://orcid.org/0000-0001-7343-6612
Chuanming Li
https://orcid.org/0000-0002-4006-9411

Funding Statement
This study was supported by the Chongqing Science and Health Joint Medical Research Project of China, Grant/Award Number: 2018ZDXM005; the Chongqing Natural Science Foundation, Grant/Award Number: cstc2020jcyj-msxmX0044; the Kuanren Talents Program of the Second Affiliated Hospital of Chongqing Medical University, Grant/Award Number: 2020-7.

Acknowledgments
We are grateful for the research volunteers, their families, and the investigators at the Alzheimer's Disease Neuroimaging Initiative (ADNI) database. ADNI is funded by the National Institute on Aging, the National Institute of Biomedical Imaging and Bioengineering, and through generous contributions from the following: AbbVie, Alzheimer's Association; Alzheimer's Drug Discovery Foundation; Araclon Biotech; BioClinica, Inc.; Biogen; Bristol Myers Squibb Company; CereSpir, Inc.; Cogstate; Eisai Inc.; Elan Pharmaceuticals, Inc.; Eli Lilly and Company; EuroImmun; F. Hoffmann-La Roche Ltd. and its affiliated company Genentech, Inc.; Fujirebio; GE Healthcare; IXICO Ltd.; Janssen Alzheimer Immunotherapy Research & Development, LLC.; Johnson & Johnson Pharmaceutical Research & Development LLC.; Lumosity; Lundbeck; Merck & Co., Inc.; Meso Scale Diagnostics, LLC.; NeuroRx Research; Neurotrack Technologies; Novartis Pharmaceuticals Corporation; Pfizer Inc.; Piramal Imaging; Servier; Takeda Pharmaceutical Company; and Transition Therapeutics. The Canadian Institutes of Health Research is providing funds to support ADNI clinical sites in Canada. Private sector contributions are facilitated by the Foundation for the National Institutes of Health(www.fnih.org). The grantee organization is the Northern California Institute for Research and Education, and the study is coordinated by the Alzheimer's Therapeutic Research Institute at the University of Southern California. ADNI data are disseminated by the Laboratory for Neuro Imaging at the University of Southern California.
The authors thank the application engineers Ying Pei and Huan Liu at GE Medical Systems Corporation for their assistance with MR image postprocessing; and to American Journal Experts (AJE) for their assistance with language editing.

REFERENCES

1. Hou Y, Dan X, Babbar M, Wei Y, Hasselbalch SG, Croteau DL, et al. Ageing as a risk factor for neurodegenerative disease. *Nat Rev Neurol* 2019;15:565-581
2. No authors listed. 2020 Alzheimer's disease facts and figures. *Alzheimers Dement* 2020;16:391-460
3. Ngandu T, Lehtisalo J, Solomon A, Levälahti E, Ahtiluoto S, Antikainen R, et al. A 2 year multidomain intervention of diet, exercise, cognitive training, and vascular risk monitoring versus control to prevent cognitive decline in at-risk elderly people (FINGER): a randomised controlled trial. *Lancet* 2015;385:2255-2263
4. Crous-Bou M, Minguillón C, Gramunt N, Molinuevo JL. Alzheimer's disease prevention: from risk factors to early intervention. *Alzheimers Res Ther* 2017;9:71
5. Jack CR Jr, Bennett DA, Blennow K, Carrillo MC, Dunn B, Haeberlein SB, et al. NIA-AA research framework: toward a biological definition of Alzheimer's disease. *Alzheimers Dement* 2018;14:535-562
6. Hwang J, Jeong JH, Yoon SJ, Park KW, Kim EJ, Yoon B, et al. Clinical and biomarker characteristics according to clinical spectrum of Alzheimer's disease (AD) in the validation cohort of Korean Brain Aging Study for the Early Diagnosis and Prediction of AD. *J Clin Med* 2019;8:341
7. Devanarayan P, Devanarayan V, Llano DA; Alzheimer's Disease Neuroimaging Initiative. Identification of a simple and novel cut-point based cerebrospinal fluid and MRI signature for predicting Alzheimer's disease progression that reinforces the 2018 NIA-AA research framework. *J Alzheimers Dis* 2019;68:537-550

https://doi.org/10.3348/kjr.2021.0323

8. Illán-Gala I, Pegueroles J, Montal V, Vilaplana E, Carmona-Iragui M, Alcolea D, et al. Challenges associated with biomarker-based classification systems for Alzheimer's disease. *Alzheimers Dement (Amst)* 2018;10:346-357
9. Altomare D, de Wilde A, Ossenkoppele R, Pelkmans W, Bouwman F, Groot C, et al. Applying the ATN scheme in a memory clinic population: the ABIDE project. *Neurology* 2019;93:e1635-e1646
10. Ebenau JL, Timmers T, Wesselman LMP, Verberk IMW, Verfaillie SCJ, Slot RER, et al. ATN classification and clinical progression in subjective cognitive decline: the SCIENCe project. *Neurology* 2020;95:e46-e58
11. Calvin CM, de Boer C, Raymont V, Gallacher J, Koychev I; European Prevention of Alzheimer's Dementia (EPAD) Consortium. Prediction of Alzheimer's disease biomarker status defined by the 'ATN framework' among cognitively healthy individuals: results from the EPAD longitudinal cohort study. *Alzheimers Res Ther* 2020;12:143
12. Lehmann M, Rohrer JD, Clarkson MJ, Ridgway GR, Scahill RI, Modat M, et al. Reduced cortical thickness in the posterior cingulate gyrus is characteristic of both typical and atypical Alzheimer's disease. *J Alzheimers Dis* 2010;20:587-598
13. de Jong LW, van der Hiele K, Veer IM, Houwing JJ, Westendorp RG, Bollen EL, et al. Strongly reduced volumes of putamen and thalamus in Alzheimer's disease: an MRI study. *Brain* 2008;131:3277-3285
14. Cho H, Kim JH, Kim C, Ye BS, Kim HJ, Yoon CW, et al. Shape changes of the basal ganglia and thalamus in Alzheimer's disease: a three-year longitudinal study. *J Alzheimers Dis* 2014;40:285-295
15. Langa KM, Levine DA. The diagnosis and management of mild cognitive impairment: a clinical review. *JAMA* 2014;312:2551-2561
16. Vos SJ, Verhey F, Frölich L, Kornhuber J, Wiltfang J, Maier W, et al. Prevalence and prognosis of Alzheimer's disease at the mild cognitive impairment stage. *Brain* 2015;138:1327-1338
17. Ekman U, Ferreira D, Westman E. The A/T/N biomarker scheme and patterns of brain atrophy assessed in mild cognitive impairment. *Sci Rep* 2018;8:8431
18. McKhann G, Drachman D, Folstein M, Katzman R, Price D, Stadlan EM. Clinical diagnosis of Alzheimer's disease: report of the NINCDS-ADRDA Work Group under the auspices of Department of Health and Human Services Task Force on Alzheimer's Disease. *Neurology* 1984;34:939-944
19. Dubois B, Feldman HH, Jacova C, Dekosky ST, Barberger-Gateau P, Cummings J, et al. Research criteria for the diagnosis of Alzheimer's disease: revising the NINCDS-ADRDA criteria. *Lancet Neurol* 2007;6:734-746
20. Liem F, Mérillat S, Bezzola L, Hirsiger S, Philipp M, Madhyastha T, et al. Reliability and statistical power analysis of cortical and subcortical FreeSurfer metrics in a large sample of healthy elderly. *Neuroimage* 2015;108:95-109
21. Terry RD, Masliah E, Salmon DP, Butters N, DeTeresa R, Hill R, et al. Physical basis of cognitive alterations in Alzheimer's disease: synapse loss is the major correlate of cognitive impairment. *Ann Neurol* 1991;30:572-580
22. Sørensen L, Igel C, Liv Hansen N, Osler M, Lauritzen M, Rostrup E, et al. Early detection of Alzheimer's disease using MRI hippocampal texture. *Hum Brain Mapp* 2016;37:1148-1161
23. Luk CC, Ishaque A, Khan M, Ta D, Chenji S, Yang YH, et al. Alzheimer's disease: 3-dimensional MRI texture for prediction of conversion from mild cognitive impairment. *Alzheimers Dement (Amst)* 2018;10:755-763
24. Huang K, Lin Y, Yang L, Wang Y, Cai S, Pang L, et al. A multipredictor model to predict the conversion of mild cognitive impairment to Alzheimer's disease by using a predictive nomogram. *Neuropsychopharmacology* 2020;45:358-366
25. Shinde S, Prasad S, Saboo Y, Kaushick R, Saini J, Pal PK, et al. Predictive markers for Parkinson's disease using deep neural nets on neuromelanin sensitive MRI. *Neuroimage Clin* 2019;22:101748
26. Li G, Zhai G, Zhao X, An H, Spincemaille P, Gillen KM, et al. 3D texture analyses within the substantia nigra of Parkinson's disease patients on quantitative susceptibility maps and R2* maps. *Neuroimage* 2019;188:465-472
27. Geroldi C, Rossi R, Calvagna C, Testa C, Bresciani L, Binetti G, et al. Medial temporal atrophy but not memory deficit predicts progression to dementia in patients with mild cognitive impairment. *J Neurol Neurosurg Psychiatry* 2006;77:1219-1222
28. Fennema-Notestine C, Hagler DJ Jr, McEvoy LK, Fleisher AS, Wu EH, Karow DS, et al. Structural MRI biomarkers for preclinical and mild Alzheimer's disease. *Hum Brain Mapp* 2009;30:3238-3253
29. Whitwell JL, Przybelski SA, Weigand SD, Knopman DS, Boeve BF, Petersen RC, et al. 3D maps from multiple MRI illustrate changing atrophy patterns as subjects progress from mild cognitive impairment to Alzheimer's disease. *Brain* 2007;130:1777-1786
30. Masters CL, Bateman R, Blennow K, Rowe CC, Sperling RA, Cummings JL. Alzheimer's disease. *Nat Rev Dis Primers* 2015;1:15056
31. Jacobs HI, Van Boxtel MP, Jolles J, Verhey FR, Uylings HB. Parietal cortex matters in Alzheimer's disease: an overview of structural, functional and metabolic findings. *Neurosci Biobehav Rev* 2012;36:297-309
32. Horínek D, Varjassyová A, Hort J. Magnetic resonance analysis of amygdalar volume in Alzheimer's disease. *Curr Opin Psychiatry* 2007;20:273-277
33. Tang X, Holland D, Dale AM, Miller MI; Alzheimer's Disease Neuroimaging Initiative. APOE affects the volume and shape of the amygdala and the hippocampus in mild cognitive impairment and Alzheimer's disease: age matters. *J Alzheimers Dis* 2015;47:645-660
34. Golde TE, Eckman CB, Younkin SG. Biochemical detection of Abeta isoforms: implications for pathogenesis, diagnosis, and treatment of Alzheimer's disease. *Biochim Biophys Acta*

2000;1502:172-187
35. Buchhave P, Minthon L, Zetterberg H, Wallin AK, Blennow K, Hansson O. Cerebrospinal fluid levels of β-amyloid 1-42, but not of tau, are fully changed already 5 to 10 years before the onset of Alzheimer dementia. *Arch Gen Psychiatry* 2012;69:98-106
36. Jack CR Jr, Knopman DS, Weigand SD, Wiste HJ, Vemuri P, Lowe V, et al. An operational approach to National Institute on Aging-Alzheimer's Association criteria for preclinical Alzheimer disease. *Ann Neurol* 2012;71:765-775
37. Sonnen JA, Larson EB, Crane PK, Haneuse S, Li G, Schellenberg GD, et al. Pathological correlates of dementia in a longitudinal, population-based sample of aging. *Ann Neurol* 2007;62:406-413
38. James BD, Wilson RS, Boyle PA, Trojanowski JQ, Bennett DA, Schneider JA. TDP-43 stage, mixed pathologies, and clinical Alzheimer's-type dementia. *Brain* 2016;139:2983-2993

https://doi.org/10.3348/kjr.2021.0323